

PAPER • OPEN ACCESS

Preliminary results on surface treatments on wood

To cite this article: L de Ferri *et al* 2020 *IOP Conf. Ser.: Mater. Sci. Eng.* **949** 012094

View the [article online](#) for updates and enhancements.

Preliminary results on surface treatments on wood

L de Ferri¹, M Strojecki², C Bertolin¹

¹ Department of Mechanical and Industrial Engineering, Norwegian University of Science and Technology, Richard Birkelands vei 2b, 7491 Trondheim, Norway.

² Jerzy Haber Institute of Catalysis and Surface Chemistry, Polish Academy of Sciences, Niezapominajek 8, 30-239 Cracow, Poland

Abstract. One of the main issues of the international research project SyMBoL - Sustainable Management of Heritage Buildings in a Long-term perspective, is the evaluation of wood mechanical properties. Particularly, pine wood is tested being the main building materials of medieval Norwegian stave churches. Experiments are aimed to assess variations in mechanical properties as a function of environmental conditions. Being wood highly sensitive to RH% changes, pine slices were maintained at 80% RH (4 weeks, 20°C) and successively treated with the materials here discussed on the two main surfaces; afterward, they were left at 30% RH for three weeks. Thus, the loss of water from the samples is supposed to occur only through the lateral surfaces since the chosen sealing materials were selected on the basis of their capability to avoid any penetration of water into the samples. This work represents, indeed, the study carried out to select materials to be applied on the wooden surfaces. Paraloid B72, also coupled with a cellulose sand seal spray, a microcrystalline wax and an epoxy resin were tested. Obtained surfaces were evaluated in term of water repellency (contact angle measurements), uniformity of the surface; penetration of the materials into the wooden structures, colour and water vapor sorption.

1. Introduction [1]

Cellulose is one of the major constituents of the wood cell wall and is a highly hygroscopic material gaining or losing moisture depending on the environmental relative humidity (RH) conditions. The so-called equilibrium moisture content (EMC) can be defined as the moisture content reached when wood is exposed to given temperature and RH values, which is defined as the fraction or percentage of saturation of the surrounding water vapour. Sorption isotherms are characteristic graphs relating the EMC to various RH at a fixed temperature (T). In case of wood, sorption isotherms have quite generally a sigmoid appearance, which is concave at low RH and convex at high RH.

Wood is one of the most diffuse materials used for the creation of objects and architectural structures of artistic and anthropological interest. Wooden items can be easily found as support for paintings, statues, furnishings, musical instruments, coaches, ships, or architectural elements. Artworks have been realized using different wooden species depending on the geographical area, on the historical period and on the building and/or carving expertise. In the northern Europe countries Pine wood is one the most often employed materials for historical buildings, together with spruce wood.

Wood is in its fully saturated state if all cell cavities are filled by liquid water and cell walls are saturated by water molecules adsorbed within the fibrillar structure. Consequently, in this condition both bound water - adsorbed on the cell walls, and liquid or lumen water - in the voids of the wood microstructure, exists.

This fully saturated state is typical of the “green” wood of living trees, but it can also be produced in laboratory by soaking a wood specimen with water. If environmental RH decreases, water tends to



gradually escape from the microscopic structure, initially from cavities that get progressively empty. This state corresponds to the Fiber Saturation Point (FSP), being the EMC at which the cell walls are still saturated, but no liquid water remained in the lumens. The most of liquid water is lost for RH values lower than 60%, so further decreases in environmental RH induces the loss of bound water.

Dimensional changes are the most evident effects of moisture sorption/desorption experienced by wood since it shrinks when losing moisture and swells when gaining moisture. Furthermore, wood is an anisotropic material and dimensional changes are generally different in all three anatomical directions, i.e. longitudinal, tangential and radial. The smallest dimensional response is observed along the longitudinal direction while the highest is observed along the tangential one. These dimensional changes are also closely related to changes of the wood mechanical properties, affected by the fiber's hydration. Such variations in term of RH are quite easily experienceable in historical buildings since the presence or absence of heating systems can strongly affect the indoor microclimate. When considering wood-based historical structures in the Northern Europe heating systems are never present in civil building such as the typical wooden house protected in open-air museums and rarely installed in original warehouses (sometimes only few rooms are heated). Stave churches are probably the most famous Norwegian historical structures: being the indoor climate conditions directly dependent on the external ones, heating systems were installed starting from 1897 when a law imposed the mandatory heating of churches in order to make the environments more comfortable for visitors and patrons. Newer heating systems were installed in most churches during the 20th century.

Conservation plans for such historical sites generally foresee the replacement of excessively degraded materials with new ones and, only for stave churches the treatment (every 10 years) of external surfaces with tar. Explorative studies carried out in a warehouse in Trondheim evidenced that the new logs used for replacements have been treated applying an undefined conservative treatment [2]. Therefore, a series of experiments has been planned in the frame of the international research project SyMBoL - Sustainable Management of Heritage Buildings in a Long-term perspective to study the influence of various surface treatments of wood on its sorption properties.

The presented work presents, indeed, the results obtained by testing sealing materials deposited on wooden samples in order to determine the most suitable treatments to be used in further experiments foreseeing the induced moisture penetration and loss only through the lateral surfaces of pine slices in order to finally get information concerning modification in the mechanical properties of treated pine-wood samples submitted to strong RH variations.

2. Material and Methods

2.1 The samples

Pine wood slices (20 x 10 x 2 cm) were obtained from radial cut by a log naturally dried in open environmental conditions in the Trøndelag area, Norway, for ~3 years (figure 1). The log was then transported into the laboratory with ~23 °C and 24% RH and acclimatized there for 3 months. Slices were obtained from a wood cut at 34 cm depth with respect to the log external radial surface.

Fully saturated pine wood slices are foreseen to be kept in high RH conditions (80%) for 4 weeks at constant temperature and then treated with coating materials on two main (radial) surfaces. In this way it is assumed that further exchanges of moisture with controlled environmental conditions could be limited and may occur only through the lateral surfaces. Successively, treated slices will be maintained for 4 weeks at 30% RH, in order to induce a loss of moisture and finally verify variations in the wood mechanical properties with respect to materials kept at standard room conditions for the entire period.

Chemicals described in section 2.2 were tested and obtained surfaces were characterized as indicated in section 2.3.

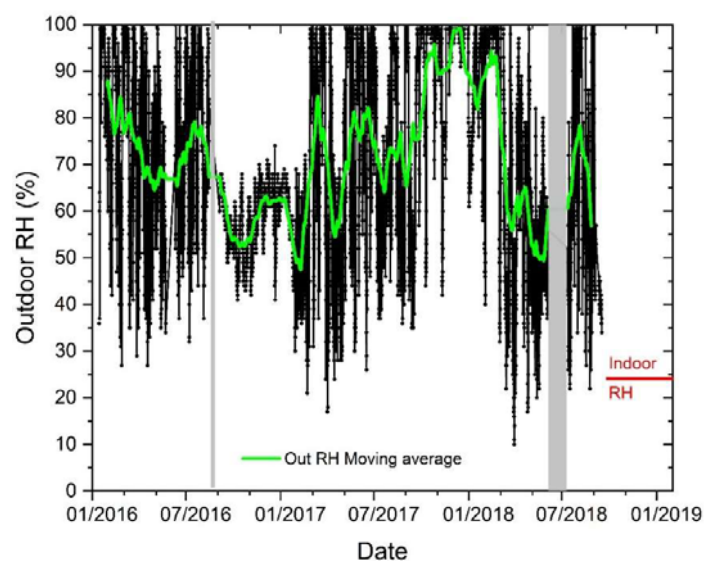


Figure 1. Environmental relative humidity (%) oscillation and running average (green line) to which the pine wood log has been exposed between 2016 and 2018.

2.2 The treatments

A 40% (w/v) solution of Paraloid B72 (Phase) in acetone (Sigma Aldrich) was prepared at 60°C in a closed container under magnetic stirring (80 rpm) in order to speed up the polymer dissolution. The Paraloid solution (P40) was deposited by brush on the wooden surface. Additionally, its coupling with a cellulose sand seal spray (Verktøy AS-CS), commonly employed in the preparation of wooden materials in order to avoid water capillary rise, was tested. CS was sprayed on the pine wood surface and let dry for 5 min before depositing the P40 solution. Another sample coated only by CS was also prepared. Further tested materials were the Reinassence (R) microcrystalline wax, used by many European museums on different materials, including wood, and a fast drying (5 min) epoxy resin (E). These last two products were deposited by means of a spatula.

2.3 Characterization

Surface homogeneity, penetration of the chemicals and treatments thickness were evaluated by optical microscopy by means of a Dino Edge-Digital programmable optical microscope, acquiring images at different magnifications (from 20 to 200x). Furthermore, SEM images were captured by using a Quanta 650 ESEM (Thermo Fisher) working in low vacuum conditions.

The effect of the coatings on the optical appearance of the wood was measured according colorimetric standards. Two methodologies i.e. the Natural Color System (NCS) and CIE $L^*a^*b^*$ system were adopted and compared. In the first case the samples were analyzed by the X-Rite Capsure RM200QC spectrophotometer quickly capturing exact colorimetric from any source, even patterned and textured surfaces. The X-Rite Capsure integrates with Pantone color libraries auto-extracting the dominant color and giving also the related CIE $L^*a^*b^*$ values. The instrument utilized a 45°/0° measurement geometry on a Ø=9 mm spot by means of VIS and UV LED sources. Measurements were taken resting this very small and light instrument on the surface of the samples, being the optical system totally integrated, it did not necessitate of any adjustment.

Parallel, spectral images of wood samples were acquired by means of a spectrophotometric scanner [3] using a CIE Standard illuminant D_{65} . It is a standard illuminant, being a theoretical source of visible light, whose spectral power distribution is known. Illuminants from series D are built to represent natural daylight and D_{65} roughly resembles the average midday light in Western / Northern Europe (including both direct sunlight and light diffused by a clear sky), for this reason it is also called a daylight illuminant.

As a reference, the white certified standard was used, in the same optical geometry as for the image acquisition ($45^\circ/0^\circ$). Measures were performed in a total dark environment in order to avoid noise due to external light sources. Samples were placed together on a flat perfectly white surface setting the focal distance of the camera in order to obtain perfectly focused spectral images. The distance was calibrated by means of a set of three standard samples displaying b/w patterns at increasing density. The camera, set between the two employed light blades, moves scanning the whole set of samples and acquiring the total spectral image. Finally, regions of interests (ROI) can be selected through the proprietary software: on every sample 3 ROIs in the dark brown and 3 ROIs in the light areas were selected. For every selected ROI color coordinates in the CIE $L^*a^*b^*$ space from the spectral reflectance factor of every pixel of the image were obtained. Mean values of L^* (lightness), a^* (redness) and b^* (yellowness) data acquired in three points from treated and untreated samples were used to obtain both the average color difference ΔE^*_{76} [3-5] and $CMC_{(2:1)}$ [6], as defined in eq. (1) and (2):

$$\Delta E^* = \sqrt{\Delta L^{*2} + \Delta a^{*2} + \Delta b^{*2}} \quad (1)$$

$$\Delta E_{CMC} = \sqrt{\left(\frac{\Delta L^*}{S_L}\right)^2 + \left(\frac{\Delta C^*}{cS_c}\right)^2 + \left(\frac{\Delta H}{S_H}\right)^2} \quad (2)$$

Where $l=2$ and $c=1$, S_L is defined as in eq. (3) since for the investigated samples L^* is always > 16 :

$$S_L = \frac{0.040975 \cdot L_1^*}{1 + 0.01765 \cdot L_1^*} \quad (3)$$

where L_1^* is the lightness value of the untreated sample. S_c is defined as in eq. (4):

$$S_c = \frac{0.0638 \cdot C_1^*}{1 + 0.01313 C_1^*} + 0.638 \quad (4)$$

S_H is defined as in eq (5):

$$S_H = S_c(FT + 1 - F) \quad (5)$$

Where F is defined as in eq. (6):

$$F = \sqrt{\frac{C_1^{*4}}{C_1^{*4} + 1900}} \quad (6)$$

and T as in eq. (7) being $h_1 < 164^\circ$ for all the samples:

$$T = 0.36 + |0.4 \cos(h_1 + 35)| \quad (7)$$

In order to calculate $CMC_{(2:1)}$ values recorded $L^*a^*b^*$ coordinates were transformed in $L^*C^*h^*$.

To evaluate the ability of wood surface for water penetration or escape the static contact angle measurements were conducted. Recommendations of the UNI 11207:2007 protocol [7]) were adapted for the wooden surface.

Samples were placed on a xyz micro-translation stage and three $5\mu\text{l}$ water droplets were deposited perpendicularly to the surface through a flat-ended needle micropipette. Droplets were illuminated from behind with an incandescent white light source and a diffuser screen. The acquisition set-up consisted of a Canon Ixus 190 digital camera. The camera was set in macro mode, placed at about 10 cm from the sample. The images were acquired in 15 s after the deposition of the droplets. Obtained images were processed in Matlab® using a custom-made graphical-user-interface program by selecting two extreme points at the base of the drop and its top point. The static contact angle θ was determined in the spherical approximation by eq. (8):

$$\theta = 2 \arctg\left(2 \frac{h}{d}\right) \quad (8)$$

where d and h are the base width and the height of the droplet, respectively.

Measurements of water vapor sorption were performed gravimetrically on the collected samples by means of a vacuum microbalance (CI Electronics Ltd), following the methodology described in Bratasz et al., 2012 [8]. Adsorption branches of the water vapor isotherms were determined later in the laboratory at room conditions ($T=24^{\circ}\text{C}$) and for a full range of water vapor relative pressures. Typically, a 0.1 g wood fragment was weighted and outgassed before performing the measurement under a vacuum of a residual pressure of less than 0.1 Pa in order to move the air out of the wood and to eliminate most of the species physisorbed during the storage of the sample, especially adsorbed water. The process was fully automated, and the measuring of 10 adsorption points took on average several hours.

3. Discussion of the Results

3.1 Optical and Electron Microscopy

Images acquired by means of optical (left side) and electron microscopy (right side) on the wooden samples treated with all the tested chemicals are shown in figure 2. As can be seen both in case of R and CS treatment sample surfaces were not significantly modified, whereas both P40 and epoxy resin are deposited more less uniformly. In these cases, glossy layers with many entrapped bubbles can be observed. SEM images allow to notice differences when Paraloid solution is deposited with or without preparatory spraying of the cellulose sand. In this last case, in fact, the surface looks smoother and a lower amount of internal tensions, seen as bright areas, are present. Furthermore, the observation of the E sample surface with an optical microscopy shows the presence of relatively high amount of material deposited in a quite inhomogeneous way. This observation can be confirmed in the SEM image, clearly presenting the preferential accumulation of the epoxy resin in some areas.

When examining the samples sections (figure 3) in visible light, no penetration of the chemical treatments could be detected. It has been observed that the application of the CS spray acted as a partial impregnation modifying the surface ability for the P40 solution penetration, resulting in thinner layer of P40 deposited (figure 3). Similar conclusion can be drawn from observation of the surfaces.

Unfortunately, SEM images of cross sections did not permit to obtain additional information about the deposited layers thicknesses, as shown in figure 3. They have been estimated from pictures acquired by means of optical microscopy and data are reported in Table 1. In case of CS the deposited layer is almost unmeasurable while the maximum thickness was found for E treatment. Moreover, the deposited layers thickness is not uniform across the samples generally due to the deposition method, highly depending on the operator.

Table 1: Thickness values of surface treatments deposited on the pine wood samples.

Surface treatment	Thickness (mm)
R	0.2-0.41
CS	n.d.
CS+P40	0.07-0.1
P40	0.3-0.35
E	0.15-0.3

3.2 Colorimetry

Data obtained in the NCS colour system were acquired by means of a handheld and relatively not expensive colour matching instrument that can quickly capture exact colour metrics and fit them to the integrated PANTONE libraries.

NCS is based on the colour opponency hypothesis of colour vision stating, that the human visual system can create colour information in an antagonistic manner. Since overlaps exist in the wavelength ranges detected by the three cones of the human eye (L for long-wave, M for medium-wave and S for short-wave light), the visual system better recognizes differences between their responses rather than cone specific functions. Consequently, three opposing colour pairs are theorized: red vs green, blue vs yellow, and black vs white (the last type is achromatic and concerns light-dark variation, or luminance) [5].

Therefore, NCS system results to be based on human perception and not on colour mixing, considering the 6 elementary colours of the opponency theory that cannot be defined by mixing each other. On the other hand, every other colour is explainable in terms of similarity to the six elementary colours [5,9]. Every colour is identified by a specific notation including letters and numbers, normally starting with *S*, indicating the NCS 1950 standard. Three numerical values express percentages of blackness (*s*, relative visual similarity to the black elementary colour), chromaticness (*c*, relative visual similarity to the most saturated colour in the hue triangle [9]) and hue (ϕ , relative similarity to one or two of the chromatic elementary colours). This second part of the colour notation can be more generally described as the colour position within the NCS colour circle. The percentage values lay between two letters indicating the elementary colours it resembles to, to a lesser extent to the first and to a greater extent to the second. In this way the NCS colour system provides an unambiguous definition of a colour permitting the description of any surface and is the reference norm for colour designation in different countries, including Norway.

Acquired data are reported in Table 2. The main limit observed for this measuring system on a textured material as wood, displaying light and dark brown areas corresponding to the succession of the growing rings, was the impossibility to systematically obtain matching for both hues. As shown in Table 2, in some cases the system recognized only average colour, while in others the two dominant hues and the average one could be detected, basically for P40 samples. In addition, the instrument gave the lightness v values (Table 2), defined in the NCS for chromatic colours by comparison to a reference scale of achromatic colours. This parameter varies between 0 and 1, corresponding to black and white, respectively. Comparing values reported in Table 2 it is noticeable that treatments maintaining the highest similarity in term of v with respect to the untreated wooden samples are CS and R. Similarities are almost confirmed by obtained $L^*a^*b^*$ (Table 2 and figure 5a) and calculated ΔE^* values (Table 3, comparing corresponding couples of data set). In particular, the lower colour difference was found when treating the wood surfaces with the cellulose sand spray, which presence is hardly detectable by naked eye (human eye can capture the difference when $\Delta E \geq 3$ [5,10]), while the highest difference was achieved when coupling it with Paraloid B72.

The effect of CS coating is almost unnoticeable when it is applied alone, whereas its presence seems to affect the colour modification when P40 is deposited, especially on the lighter areas.

$L^*a^*b^*$ parameter values are also the main output obtained from the spectrophotometric scanner (figure 5b). A comparison between this well-established bench top instrument and the simpler and portable version previously described has been attempted. Colorimetric coordinates values measured by means of the scanner are reported in Table 3 as well as the ΔE^* values obtainable by the X-Rite spectrometer. Unfortunately for this instrument colour differences could be calculated only for the P40 and CS+P40 samples, since only in these cases colorimetric data could be extracted for the light and dark component separately. As can be observed from figure 4b, acquisition by the bench top instrument provided more consistent results. Series referable to the light and dark areas of the wooden surfaces are, in fact, clearly separated and follow the same patterns. The only exception seems to be represented by the P40 samples. In this case the variation in term of a^* is much higher due to a certain variability in the values of the three collected points, which can be confirmed by the standard deviation.

Finally, the colour difference has been evaluated also considering the $CMC_{(2:1)}$ relation: in 1984 the Colour Measurement Committee (CMC) of the Society of Dyers and Colourists developed a colour difference relation that could better match the visually perceived differences with respect to the CIELAB one. The relation is reported in section 2.3 as eq. 2, based on the $L^*C^*h^*$ colour model, using polar coordinates and involving 2 new parameters with respect to the more widely known CIEL $^*a^*b^*$ space: Chroma (C^*), giving information about the colour saturation, and hue (h^*). The formula $CMC_{(t:e)}$ permitted to address perceptual nonuniformities by applying specific weight derived by tolerance tests, since tolerance for an acceptable colour match consists of a three-dimensional space with variable limits for lightness, chromaticity and hue. ΔE^* represents the easiest way to have a spherical tolerance, while the CMC formulas correspond to the equation for 3D ellipsoids with axes in the directions of ΔL^* , ΔC^* and ΔH^* [6]. It has been demonstrated that such kind of tolerance is more like the human perception reducing the extent of the disagreement between the observer and the instrumental values since human eye does not register differences in lightness, chromaticity and hue at the same way.

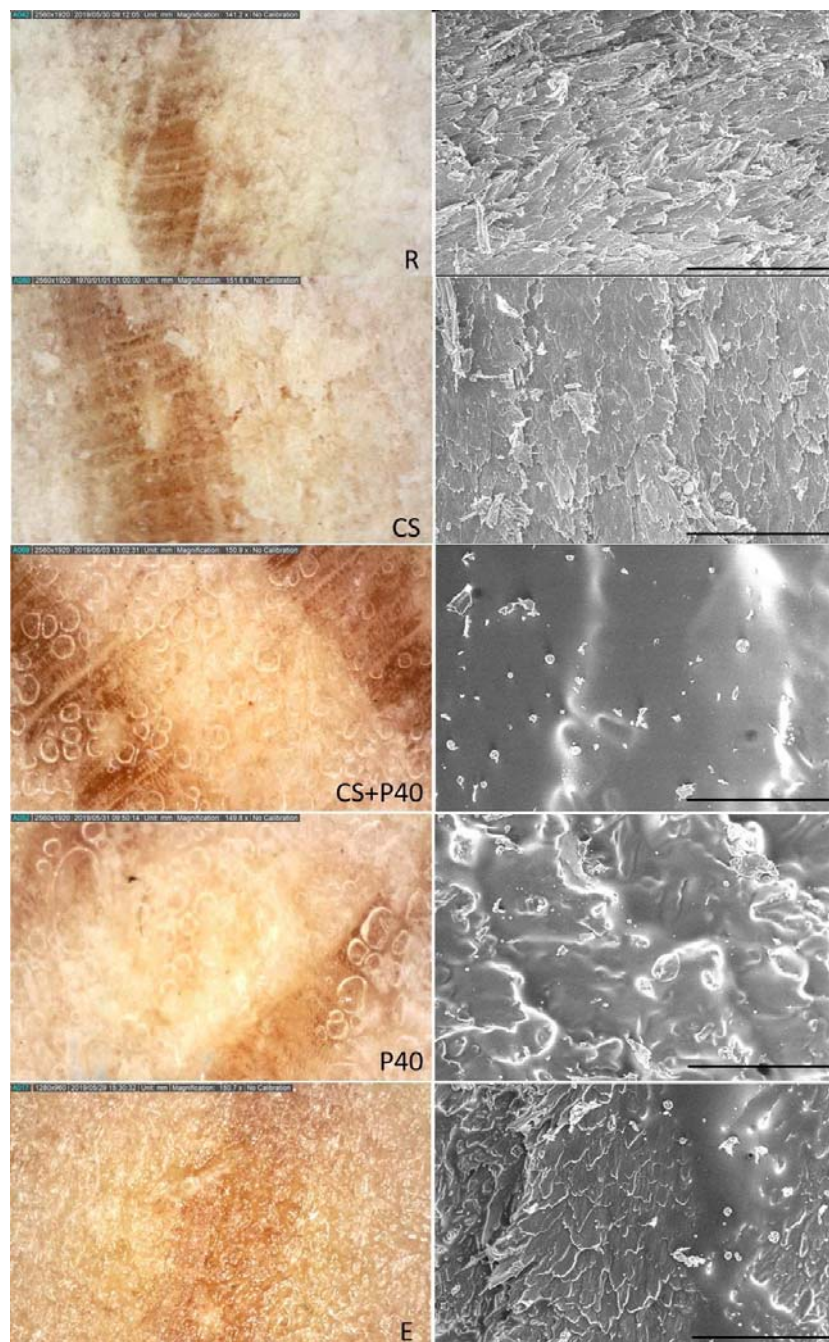


Figure 2. Optical microscopy(150x) and SEM images (secondary electrons, the black segments correspond to 300 μ m) of pine samples surfaces treated with: Reinassence microcrystalline wax (R); cellulose sand seal spray (CS); cellulose sand seal spray and Paraloid (CS+P40); Paraloid (P40); epoxy resin (E).

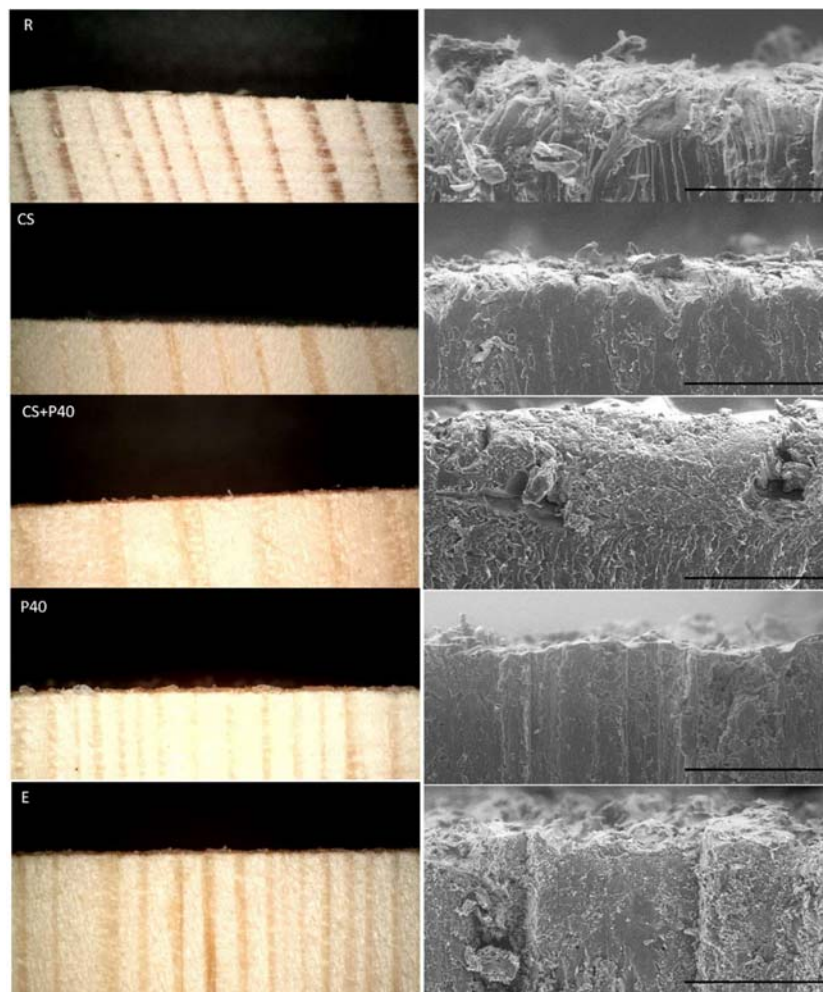












Figure 3. Optical microscopy(150x) and SEM images (secondary electrons, the black segments correspond to 300 μ m) of the cross sections of pine samples treated with: Reinassence microcrystalline wax (R); cellulose sand seal spray (CS); Paraloid (P40); cellulose sand seal spray and Paraloid (CS+P40); epoxy resin (E)

Table 2. Colour data obtained in the Natural Colour System and L*a*b* values extracted from the X-Rite Capsure spectrophotometer.

Sample	NCS	v	L*	a*	b*	
untreated light	S1510-Y30R		0.81	81.16	4.22	16.67
untreated dark	S3020-Y60R		0.59	62.83	13.22	16.36
untreated average	S2020-Y40R		0.71	72.05	11.36	22.41
P40 light	S3020-Y30R		0.62	64.49	9.81	23.77
P40 dark	S4040-Y50R		0.41	47.58	23.91	30.56

CS+P40 light	S3030-Y30R		0.59	62.07	13.95	30.27
CS+P40 dark	S4040-Y60R		0.39	45.65	26.09	28.33
CS	S2020-Y30R		0.74	74.35	9.28	24.16
R	S2010-Y40R		0.75	75.38	6.2	15.65
E	S3040-Y40R		0.53	57.08	21.84	34.22

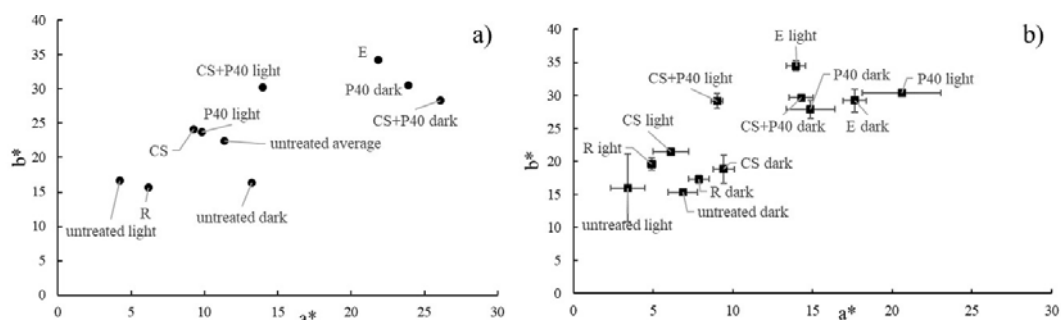


Figure 5. a^* , b^* Colour coordinates of the treated pine samples obtained through a) the X-Rite spectrometer and b) the spectrophotometric scanner.

Table 3. Color coordinates, standard deviation and color difference ΔE^* and $CMC_{(2:1)}$ values obtained through the spectrophotometric scanner. ΔE^* values calculated on the basis of data acquired obtained by the X-Rite spectrometer are reported for the P40 and CS+P40 samples.

	L^*_{av}	σ_L	a^*_{av}	σ_a	b^*_{av}	σ_b	$\Delta E^*_{scanner}$	ΔE^*_{X-Rite}	$CMC_{(2:1)}$
untreated light	76.29	2.37	3.41	1.08	15.99	5.19			
untreated dark	61.85	3.28	6.88	0.92	15.32	0.27			
R light	74.79	0.41	4.91	0.27	19.59	0.95	4.18		3.28
R dark	61.69	3.54	7.87	0.65	17.31	0.63	2.24		1.49
E light	57.07	1.38	13.96	0.62	34.48	0.82	28.68		20.86
E dark	48.64	2.16	17.64	0.71	29.21	1.71	21.99		15.25
CS light	73.27	1.37	6.11	1.13	21.47	0.39	6.82		5.60
CS dark	57.09	2.67	9.43	0.67	18.80	2.17	6.43		4.57
P40 light	63.14	0.48	20.59	16.75	30.35	0.44	25.97	18.96	25.28
P40 dark	52.97	2.58	14.88	1.52	27.92	1.34	17.38	23.42	11.68
CS+P40 light	61.55	0.39	9.01	0.38	29.16	1.15	20.54	25.38	14.37
CS+P40 dark	51.41	0.92	14.29	0.76	29.67	0.36	19.24	24.58	12.46

As a consequence, CMC is not a colour space but a tolerance system and it has been specifically designed for D_{65} illuminant. The $CMC_{(l:c)}$ equation allows to modify the ellipsoids dimensions in order to match visual acceptability and this can be done by means of the tolerance parameters l and c . They serve for weighting the lightness and hue differences and values can vary with the application field. For this study values of 2 and 1 were considered for l and c , respectively meaning the lightness contributing half as much to the difference (a twice tolerance is allowed) as the chroma [6].

When considering data reported in Table 3, differences with respect to the ΔE^* are clearly visible, being almost all the calculated values lower than those obtained by using ΔE^* . This correspond quite well to the visual perception of treated samples, in some cases appearing not so much different by the untreated ones, as in the cases of the microcrystalline wax (R) or the CS spray.

3.3. Static contact angle

The most common way to evaluate the surfaces wettability is through the measurement of the static contact angle, defined as The contact angle between a liquid and a solid is the angle geometrically determined by the tangent to the liquid drop from the contact point along the gas–liquid interface, as shown in figure 6. For static contact angle values (θ) lower than 90° a surface is defined hydrophilic since the liquid will wet the surface and spread over it; on the other hand, for $\theta \geq 90^\circ$ it is considered hydrophobic because the liquid will remain on the surface forming a more spherical drop. Therefore, the contact angle between a liquid and a solid depends on the nature of the liquid as well as the surface characteristics (chemical and morphological) of the solid [11].

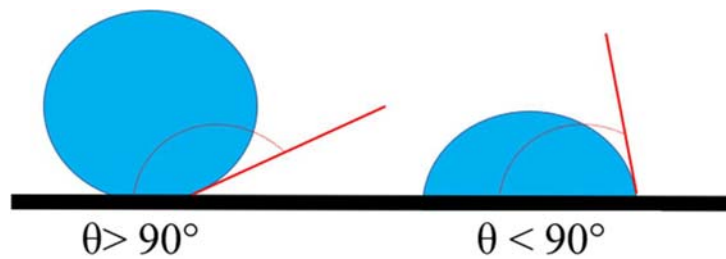


Figure 6. Contact angle of a water drop with a solid surface.

Five water droplets have been deposited on each treated sample and results are reported in Table 4 as average values. In general, obtained values only two times reach the minimum of 90° , normally indicated as a limit to define the surface as hydrophobic [11]. Notwithstanding, both the chemical properties and thicknesses of treatments CS+ P40, P40 permitted to completely avoid water penetration. In case of P40, a certain inhomogeneity seems to affect measurements. The analysis of the data presented in Table 4 shows that the highest angles have been observed for the fresh layer of CS. On the other hand, it has also been observed that the slight hydrophobic properties of such product have been lost with time., E.g. the θ value of the 6 months aged sample decreased of about 20° . Parallel, while R reached the minimum value of 90° , all the other surfaces resulted almost equivalent with values of $\sim 73^\circ$.

Table 4. Average static contact angle θ ($^\circ$) on pine wood samples treated with the different coatings after 6 months from deposition (except CS_{fresh}).

Treatment	θ ($\pm 3^\circ$)
R	90
CS	78
CS _{new}	98
CS+P40	73
P40	73
E	73

3.4. Water sorption

Sorption-desorption isotherms obtained for the treated and for untreated pine samples are shown in figure 7. The plot reports the variation of EMC as a function of p/p_0 , where p is the experimental partial water vapor pressure and p_0 its value at saturation. It can be expressed as a fraction of relative humidity in eq. 9:

$$\frac{p}{p_0} = \frac{RH}{100} \quad (9)$$

As can be seen in the graph the samples show a gradual decrease in the reached EMC values. The treatments that more affected the pine wood capability of adsorb water vapor is the epoxy resin (max ECM % value ~13%). On the contrary, the less influencing wood surfaces water vapor adsorption is the cellulose sand seal spray: the maximum reached value for the CS sample is, in fact, ~ 20% while for the untreated one is ~ 21%. Moreover, E and P40 treatments show similar sorption-desorption isotherms, although with different influence on the EMC. CS and R highlight an adsorption-desorption behavior resembling the untreated sample. Finally, results for the CS coupled with P40 treatment show an intermediate behavior.

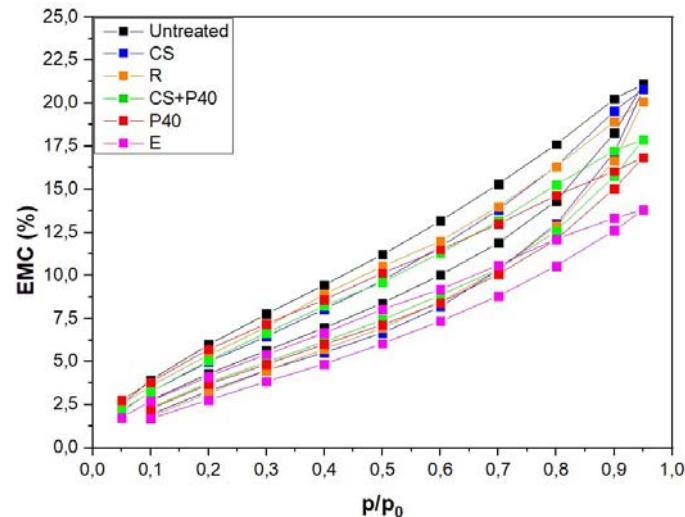


Figure 7. Adsorption-desorption isotherms of the studied specimens.

4. Conclusions

In the frame of the international SyMBoL Project, a set of pine wood samples has been treated testing different commercial sealing treatments in order to minimize the amount of water penetrating in the wood volume.

In particular, a microcrystalline wax (R), Paraloid B72 (40%), a sand sealing spray and an epoxy resin have been tested evaluating their optical appearance, the induced color change and the adsorption-desorption behavior of coated samples.

The thickest layers formed when P40 and epoxy resin have been applied on the wooden samples. The deposited film thickness was found to decrease when P40 was coupled to CS, probably due to decreased ability of further P40 solution penetration.

The highest color difference was induced by the same treatments that were also the only ones permitting the acquisition of distinct colors parameters with the X-Rite portable spectrometer. This small, inexpensive and easy to use instrument is, in fact, very effective when working on homogeneous surfaces but the identification of different colors on a patterned surface can be challenging.

As concerning the water repellency, the static contact angle measurements highlighted how none of the considered treatments displayed strong water repellency performances since only for the microcrystalline wax R the values resulted equal to 90°.

The samples adsorption of water vapor has been evaluated by means of a vacuum microbalance. The specimen showing properties similar to untreated pine wood is the one treated with microcrystalline wax, notwithstanding its quite high static contact angle. The sample covered with epoxy resin resulted in more limiting the water vapor sorption.

The results of the tests performed on the treated specimens have permitted to select the materials for the future experiments. In particular, it has been decided to utilize the microcrystalline wax (R) because of the sufficient static contact angle values shown, and the combination of sand sealing spray and Paraloid 40% permitting to obtain a barrier avoiding the penetration of water vapor with deposited layer thinner

than that obtainable when using only P40. On the other hand, epoxy resin has been excluded since the deposited film resulted very thick, induced the greatest color change and is a material only rarely utilized in the field of cultural heritage.

Acknowledgments

Authors are deeply indebted to Dr. S. M. R. Razavi (MTP department, NTNU) for the preparation of cross sections, to Dr. Di Wan (MTP department, NTNU) for acquiring SEM images of the samples, to Prof. K. Angelo (IAT Department, NTNU) for providing the X-Rite Capsure spectrophotometer, to Prof. Per Berntsen (IAT Department, NTNU) for providing the Dino microscope and Prof Solon Oikonomopoulos (Chemistry Department, NTNU) for providing the micropipette.

References

- [1] Bratasz L, 2010: Acceptable and non-acceptable microclimate variability: the case of wood. In: Camuffo D, Fassina V Havermans, eds. Basic environmental mechanisms affecting cultural heritage. Understanding deterioration mechanisms for conservation process, COST Action D 42. Chemical interactions between cultural artefacts and indoor environment. p. 49.
- [2] Bertolin C, de Ferri L, Grottesi G, Strojceki M, 2020, *Wood Sci. Technol.* **54** 203-226.
- [3] Antonioli G, Fermi F, Oleari C, Reverberi R, 2004, Spectrophotometric scanner for imaging of paintings and other works of art, Proceed. CGIV 2004 - Second European Conference on Color in Graphics, Imaging and Vision, Aachen Germany.
- [4] Briggs J C, Forrest D J, Tse M K, 1998, Canada Reliability Issues for Color Measurement in Quality Control Applications, IS&T's NIP14 International Conference on Digital Printing Technologies, Toronto.
- [5] Oleari C, 1998, Misurare il colore. U. Hoepli, Milano.
- [6] Klein G A 2010, Industrial Color Physics, Springer.
- [7] UNI 11207:2007 Protocol, "Cultural heritage - Natural and artificial stones - Determination of static contact angle on laboratory specimens".
- [8] Bratasz Ł, Kozłowski R, Kozłowska A, Rachwał B, 2012, *Eur J Wood Wood Prods*, **70** 445.
- [9] Hård A, Sivik L, Tonnquist G, 1996, *Color Res Appl* **21** 180
- [10] Sacevičienė V, Jucienė M, Dobilaitė V, Krylova V, Žalenkienė S, Dukštienė N, Bliudžius R, 2019, *J. Appl. Polym. Sci.*, **47** 523.
- [11] Letey J, Carrillo M L K, Pang X P, 2000, *J Hydrol* **231–232** 61–65.